Ain Shams Engineering Journal (2013) 4, 685–699

Ain Shams University

Ain Shams Engineering Journal

www.elsevier.com/locate/asej
www.sciencedirect.com

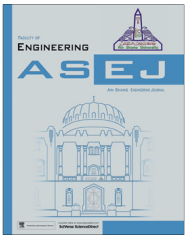

CIVIL ENGINEERING

Behavior of I-beam bolted extended end-plate moment connections

Abdelrahim Khalil Dessouki, Ahmed Hassan Youssef, Mohamed Mostafa Ibrahim *

Structural Engineering Department, Faculty of Engineering, Ain Shams University, Cairo, Egypt

Received 25 June 2012; revised 17 February 2013; accepted 11 March 2013
Available online 9 May 2013

KEYWORDS

End-plate connection;
Bolted connection;
Beam splice;
Beam-to-column connection;
Pretensioned bolts;
Moment connections

Abstract Pretensioned extended, bolted end-plate moment connections are very popular due to ease of fabrication and erection. In order to identify the effect of different parameters on the behavior of the connection, a three-dimensional finite element model that accounts for both geometrical and material non-linearities is developed using the multi-purpose software package ANSYS. A parametric study is conducted using this model on two end-plate configurations: four bolts and multiple row extended end plates. The studied parameters were as follows: beam depth, end-plate thickness, bolts diameter, bolts pitch, bolts gage, and end-plate stiffener. Then, yield line analysis is used to propose equations for the end-plate bending capacity. A design model is assumed for bolt forces analysis, and design equations are proposed. The proposed equations are compared to the finite element results and the current design codes.

1. Introduction

Over the years, end-plate moment connections have become more popular due to ease of fabrication and erection. It became the most widely used connection in the construction of metal buildings and steel portal frames. The primary use of bolted end-plate moment connections is to connect a beam-to-column or to splice two beams together, as shown in Fig. 1.

Beginning in the 1960s, research in bolted connections proved liability of bolted connections to serve as moment resisting connections. Krishnamurthy [1] had one of the earliest finite element researches where design equations were developed which lead to much thinner end plates than previously obtained by empirical formulas. Kennedy et al. [2] presented a design procedure for T-stub connections which was employed with or without modifications in most of subsequent researches. Borgsmiller [3] set a threshold that prying forces start when the applied moment on a connection reaches 90% of the end-plate capacity. Also, simplified design procedures were presented for nine end-plate configurations using yield line analysis and a modified T-stub. Bahaari and Sherbourne [4,5] constructed three-dimensional finite element model utilizing non-linear material properties to model T-stub connections and end-plate connections to unstiffened column. Mays [6] used yield line analysis to develop design procedures for the

* Corresponding author.
E-mail addresses: dessouki_ceo@hotmail.com (A.K. Dessouki), a_h_yousef69@yahoo.com (A.H. Youssef), m.mostafa.meg@gmail.com (M.M. Ibrahim).

Peer review under responsibility of Ain Shams University.

Production and hosting by Elsevier

2090-4479 © 2013 Ain Shams University. Production and hosting by Elsevier B.V. All rights reserved.
http://dx.doi.org/10.1016/j.asej.2013.03.004

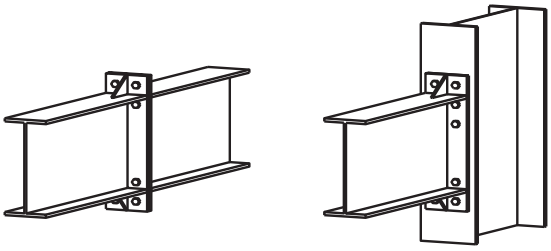

Figure 1 Bolted extended end-plate moment connection.

unstiffened column flange that showed good correlation with finite element and experimental results. Sumner [7] performed both monotonic and cyclic tests on extended end-plate moment connections which showed that the four bolts extended unstiffened and the eight bolts extended stiffened end-plate moment connections meet the requirements for use in seismic regions. Hassan [8] used 2D finite element modeling to propose reduction factors for the end-plate thickness required by the ECP-2001 [9]. Samaan [10] performed an experimental program using 10 extended and flush end-plate configurations then widened the research using a finite element model. Statistical regression analysis was used to produce equations and charts to be used for the design.

In this paper, a finite element analysis is presented to model the non-linear behavior of the extended end-plate moment connections. This model is used to conduct a parametric study on two end-plate configurations: four bolts and multiple row extended end plates. The studied parameters are as follows: beam depth, end-plate thickness, bolts diameter, bolts inside and outside pitch, inner bolts pitch, bolts gage, and end-plate stiffener. During the study, the distribution of stresses in the end plates is monitored for different configurations, and yield line patterns are observed for each configuration. These yield line patterns are analyzed and new design equations are proposed. The proposed equations are then compared to the finite element analysis results and to the current design codes equations.

2. Finite element modeling

In this study, the commercially available finite element software ANSYS [11] was used to develop the model shown in Figs. 2 and 3. The model is composed of a simply supported

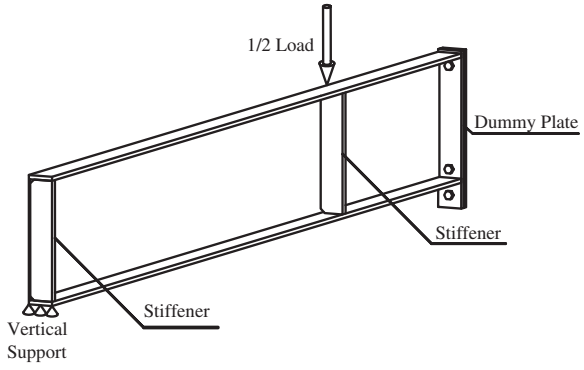

Figure 2 Schematic drawing of the finite element model (¼ of the specimen).

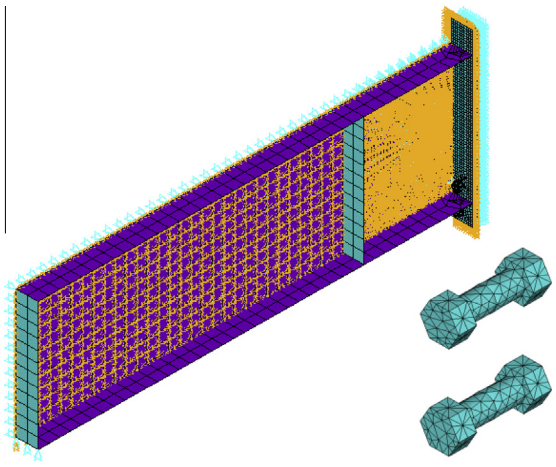

Figure 3 Finite element model.

beam spliced at mid-span with an extended end-plate moment connection. Two equal concentrated loads are applied at equal distances from splice in order to induce pure bending moment on the connection. Stiffeners are used at the locations of concentrated loads and supports to distribute the load and reduce stress concentration. In the finite element model, advantage is taken of symmetry about both the beam web and the mid-span plane (the plane passing between the two end plates) where a new dummy plate is used to simulate the contact between the existing end plate and the omitted end plate. A one quarter model of the specimen is used in the finite element model. The finite element model details are described in the following subsections.

2.1. Modeling of beam, end plate, and bolts

All steel plates including beam flanges, web, end plates, and stiffeners are modeled using four-node shell elements (SHELL181) that include plasticity effects. Solid 20-node brick elements (SOLID95) that include plasticity effects are used to model the bolts to account for biaxial stresses induced on bolts [6]. The bolts mesh is cut at the bolt shank into two separate parts, and pretension elements (PRETS179) are inserted in between to apply the pretension forces.

2.2. Modeling of end plate to end-plate contact and bolt head to end-plate contact

Contact problems present two significant difficulties: First, regions of contact are not generally known until the problem is run. Depending on the loads, material, boundary conditions, and other factors, surfaces can come into and go out of contact with each other in a largely unpredictable and sudden manner. Second, most contact problems need to account for friction. In case of pure bending moment on the connection, there is no need to account for friction in the model, so the contact surface is considered a rough surface (no slippage between contact surface and target surface). Pairs of contact and target elements (CONTA174 and TARGE170) overlaying contact surfaces mesh are used to model the non-linear contact behavior. Contact elements are constrained against penetrating the target surface. Target elements can penetrate through the contact surface. However, the contact elements are given

stiffness 10 times the stiffness of the end plate to minimize the relative displacements between surfaces. For the first contact (end plate to dummy plate), the dummy plate is the target surface and the end plate is the contact surface while in the second contact (bolt head to end plate), the end plate is the target surface and the bolt head is the contact surface.

2.3. Material properties

All materials use Von-Mises yield criterion coupled with isotropic work hardening assumption. A trilinear stress strain curve is used to define material properties [4]. The material used for the beam, end plate, and stiffeners uses the curve in Fig. 4, while material for high strength bolts uses the curve in Fig. 5.

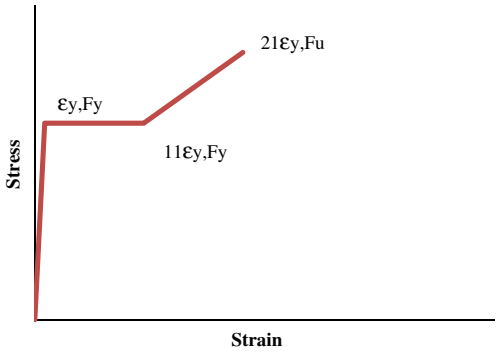

Figure 4 Stress–strain curve for beam, end plates, and stiffeners material.

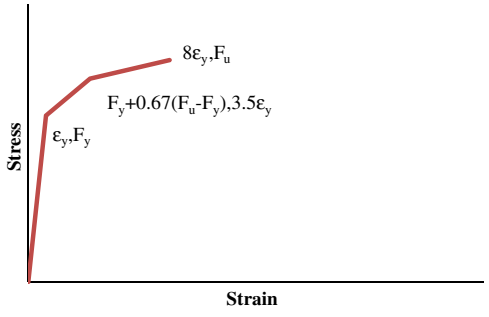

Figure 5 Stress–strain curve for bolts material.

2.4. Loads and boundary conditions

All nodes on the planes of symmetry (beam web and dummy plate) are restrained against out of plane translation and in plane rotations about both in plane axes. Also, all nodes on the bottom beam flange at the beam end are restrained against vertical translations. The loads are applied using two load steps where in the first step, pretension forces are applied to specified pretension sections in the bolts shank; then, the load step is solved, and the joints displacements from this load step are locked and applied as constant displacement in the second load step. In the second load step, the additional applied loadings alter the effect of the initial load value, but because locking transforms the load into a displacement, it preserves the initial load's effect. The second load step is then solved and the load is increased until the model becomes unstable due to excessive inelastic behavior of the structure. The "Newton–Raphson" approach is employed to solve for non-linearities. To obtain good accuracy and reasonable run time, the maximum load increment is set to be 10% of the applied load and the minimum load increment is set to 0.5% of the applied load.

2.5. Verification of finite element model

In order to verify the finite element model described formerly, it was used to model six multiple row extended end-plate connections tested by Sumner [7]. The finite element model results are compared to the reported experimental results in terms of moment capacity, moment against mid-span deflection, moment against end-plate separation (explained later in clause 4), and bolts response. From Table 1 and Figs. 6 and 7, the

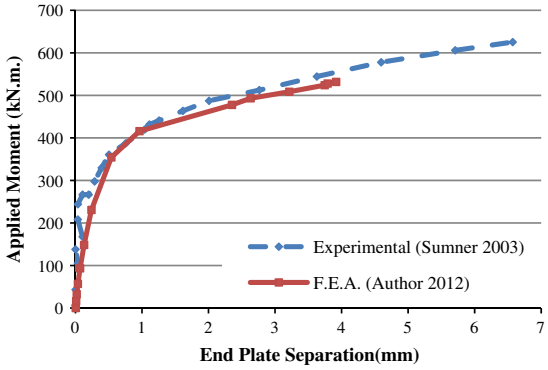

Figure 6 Test A MRE1/2-3/4-3/8-30 applied moment vs. end-plate separation.

Table 1 Comparison between experimental and F.E.A. moment capacity.

Test identification	Experimental by Sumner [7] (kN m)	F.E.A by author 2012 (kN m)	Ratio F.E.A./ experimental
Test A-MRE 1/2-3/8-3/4-30	626	530	0.85
Test B-MRE 1/2-3/4-3/4-30	857	813	0.95
Test B1-MRE 1/2-3/8-3/4-30	1015	910	0.90
Test C-MRE 1/2-3/4-1/2-30	652	661	1.01
Test D-MRE 1/2-3/4-3/4-30	756	694	0.92
Test D1-MRE 1/2-3/4-3/4-30	845	799	0.95
	Mean		0.93
	Standard deviation		0.06

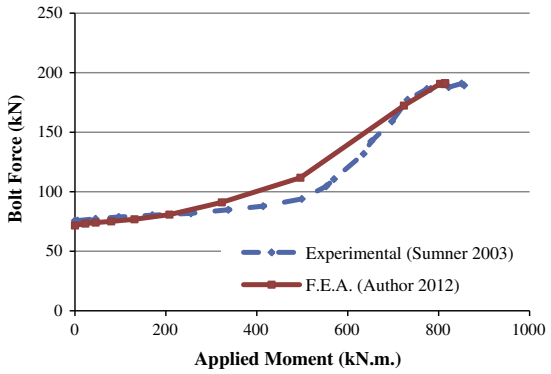

Figure 7 Test B MRE1/2-3/4-3/4-30 bolt 3 force vs. applied moment.

finite element model results have shown good correlation with the experimental results both qualitatively and quantitatively and were proven to simulate the behavior of the connection effectively. The test identification naming convention in Table 1 will be described later.

3. Parametric study

An extensive parametric study using the standard specimen shown in Fig. 8 was conducted on two configurations of the extended end-plate moment connections: (a) four bolts extended end plate and (b) multiple row extended end plate (one bolts row outside tension flange and two rows inside). The studied parameters are as follows: beam depth (d), end-plate thickness (t_p), bolts diameter (d_b), bolts gage (g), bolts outside and inside pitch (p_o, p_i), bolts inner pitch (p), and presence of end-plate stiffener. As a common practice, the value of the inside and outside pitch (p_o, p_i) is always set to be equal and the value of the inner bolts pitch (p) is equal to the sum of bolts outside and inside pitches. All the bolts are pretensioned to the minimum specified pretension force in ECP-2008 [12]. Table 2 shows the standard specimen dimensions which were not changed during the study, while Table 3 shows the different parameters values used in this research.

The naming convention used for sample identification (XX–d_b–t_p–d) is a combination of the connection configuration (XX), bolt diameter (d_b), end-plate thickness (t_p), and nominal beam depth (d). The connection configurations are designated as follows:

Table 2 Standard specimen dimensions.

Parameter	Value (mm)
Beam flange width, b_f	200
Beam flange thickness, t_f	24
Beam web thickness, t_w	12
End-plate width, b_p	200
End-plate length, l_p	d + 200
Bolts grade	8.8
Beam material	Grade 52
End-plate material	Grade 37

Table 3 Different parameters values used in this research.

Parameter	Used values (mm)
Beam web depth, d	400, 500, 600, and 700
End-plate thickness, t_p	8, 12, 16, 20, 24, 28, and 32
Bolts diameter, d_b	12, 16, 20, 24, and 27
Bolts gage, g	60, 80, 100, 120, and 140
Bolts inside and outside pitch, p_i, p_o	30, 40, 50, 60, and 70
Inner bolts pitch, p	60, 80, 100, 120, and 140
End-plate stiffener thickness, t_s	0 and 12

(a) (4E) Four bolts extended end-plate moment connection.
(b) (4ES) Four bolts extended stiffened end-plate moment connection.
(c) (MRE 1/2) Multiple row (one bolts row outside tension flange and two rows inside) extended end-plate moment connection.
(d) (MRES1/2) Multiple row (one bolts row outside tension flange and two rows inside) extended stiffened end-plate moment connection.

For example, a test designation of 4E-20-20-600 indicates a four bolts extended unstiffened connection. Bolts diameter is 20 mm, a 20 mm thick end plate, and a nominal beam depth of 600 mm.

Fig. 9 shows the definition of end-plate separation at tension flange, which was monitored for each specimen in the study and plotted vs. the applied moment. Fig. 10 shows how the connection yield moment (M_y) and the connection ultimate moment (M_u) are determined from the end-plate separation curves. The connection yield moment is the intersection of the initial connection stiffness and the strain

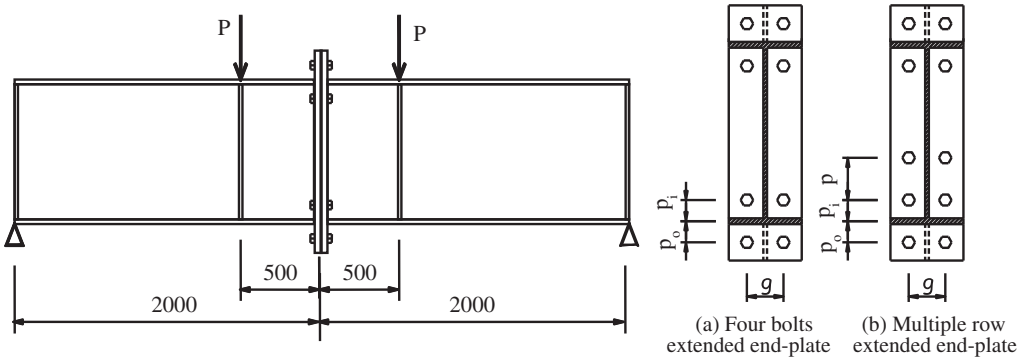

Figure 8 Standard specimen for parametric study and end-plate configurations.

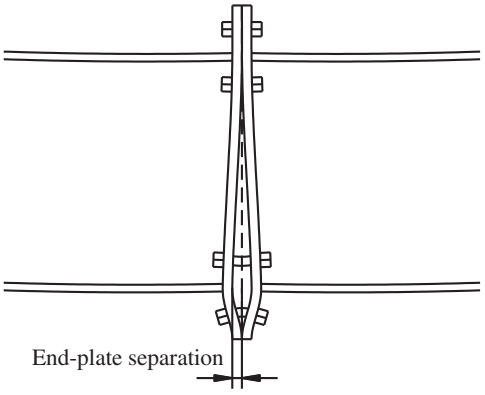

Figure 9 End-plate separation at tension flange.

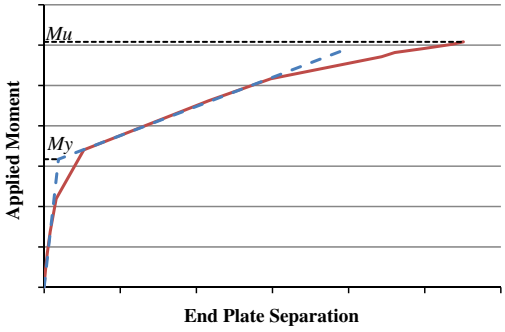

Figure 10 Connection yield and ultimate moments determined from the applied moment vs. end-plate separation curve.

hardening stiffness, where the ultimate moment is the maximum applied moment at where the model becomes unstable due to excessive inelastic behavior of the structure.

4. The behavior of extended end-plate connections

Both end-plate configurations have shown similar behavior toward the change of the studied parameter. Mainly, the study identified three types of behavior for the end-plate connection depending on the capacity of both the end plate and the bolts. Firstly, thin plate behavior where the end plate is weaker and yields before the yielding and rupture of bolts then intermediate plate behavior where end plate and bolts capacities are close and yielding of both of them occurs, and finally, thick plate behavior where the end plate is stronger and the bolts yield and rupture occurs before end-plate yielding occurs. In the intermediate plate behavior although both the end plate and bolts yielding occur, one of them occurs at first followed by the other, which makes the prior control the connection behavior. So, for simplification, the intermediate plate behavior can be neglected and the other two behaviors are considered the main types of behavior for the connection. Each of the studied parameters may affect the type of behavior the connection exhibits according to its effect on the bending capacity of the end plate or bolts. The multiple row extended end-plate configuration has shown 30–35% increase in both yield and ultimate moments than four bolts extended end-plate configuration. This increase is obviously due to increase in number of bolts in thick plate configurations, where the failure is governed by the bolts capacity. While in thin plate configurations, where failure is governed by end-plate capacity, this increase is due to the increase in number of fixation points of the end plate which leads to the formation of more plastic hinges and larger yielding capacity of the end plate.

The bolts response during the study was observed on three stages as shown in Fig. 11. At stage one, the bolt force increases slightly, the end plates are still in contact, and bolts did not lose its pretension force. At stage two, there is a sharp increase in the bolt force, and this is where end plates have lost contact and are now separated. The thinner the end plate, the sooner stage two starts due to increase in prying action which increases the force in the bolt. At stage three, the applied moment increases with little increase in the bolt force due to yielding of the bolt shank. Fig. 12 shows the end plate to end-plate contact status of sample four bolts extended end-plate connection at different load values: Just after, bolt pretension is applied and prior to application of any external load, at the connection yield moment and at connection ultimate moment. The end-plate contact status distributions show that the bottom tip of the end plates begins to be in contact before the yield moment is reached, which indicates the formation of prying forces prior to end-plate yielding in thin plate connections.

4.1. Beam depth (d)

Figs. 13 and 14 show the yield and ultimate moments for four bolts and multiple row configurations, respectively, at 12 mm and 32 mm end-plate thicknesses. As the beam depth increases from 400 to 700 mm, the yield moment is increased by about 70–80% for thin plate (12 mm) and 80–90% for thick plate

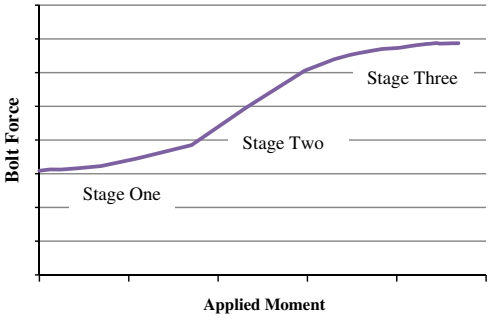

Figure 11 Typical bolt response during the study.

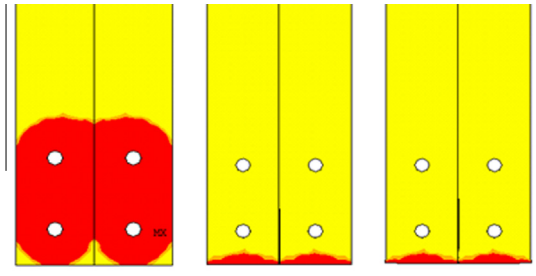

Figure 12 End-plate contact status of a sample four bolts connection.

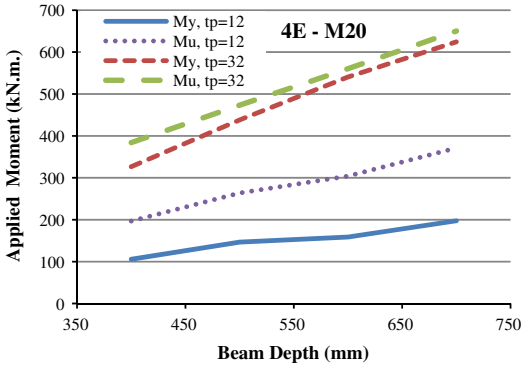

Figure 13 Yield and ultimate moments vs. beam depth at different end-plate thicknesses for four bolts configuration.

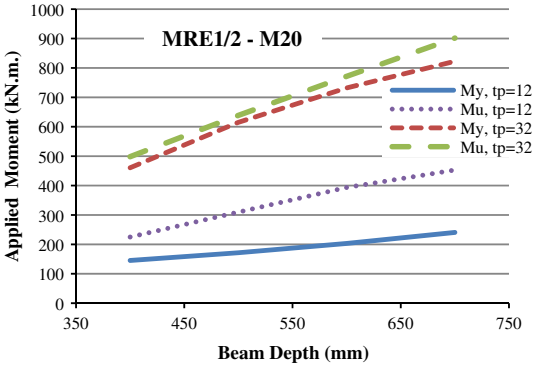

Figure 14 Yield and ultimate moments vs. beam depth at different end-plate thicknesses for multiple row configuration.

(32 mm). The connection ultimate moment increased by 80–90% for thin plate and 70–80% for thick plate.

4.2. End-plate thickness (t_p)

Figs. 15–18 show yield and ultimate moments against end-plate thickness for both four bolts and multiple row configurations. For smaller bolt diameters (M12 and M16), the connection exhibits a thin plate behavior as both M_y and M_u increase by about 225% when end-plate thickness increases from 8 mm

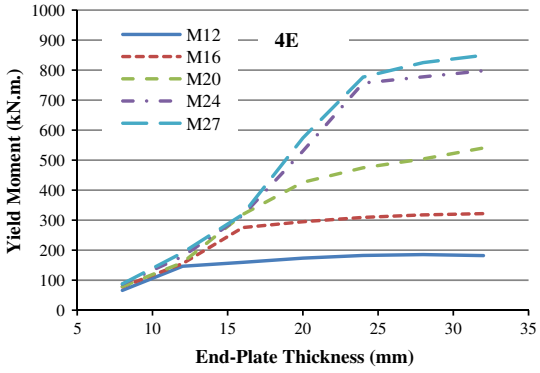

Figure 15 Four bolts configuration yield moment vs. end-plate thickness.

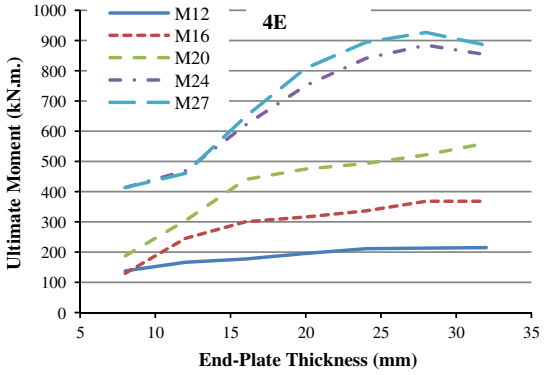

Figure 16 Four bolts configuration ultimate moment vs. end-plate thickness.

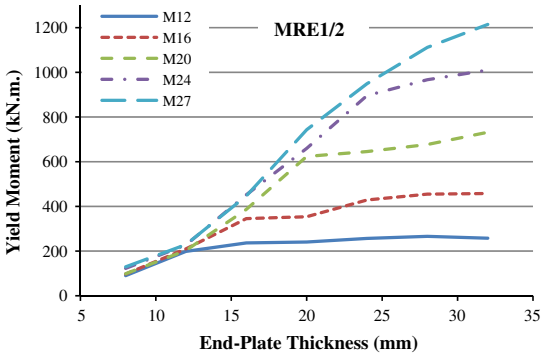

Figure 17 Multiple row configuration yield moment vs. end-plate thickness.

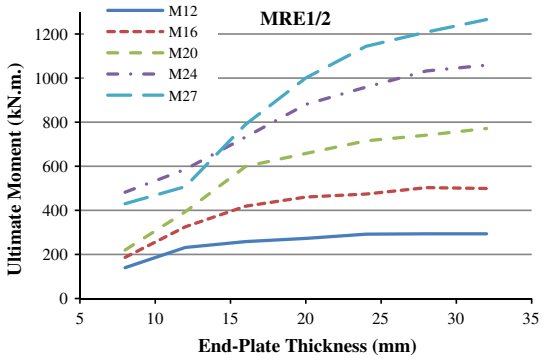

Figure 18 Multiple row configuration ultimate moment vs. end-plate thickness.

to 16 mm; then, the rate of increase is negligible as the behavior turns to thick plate behavior, and further increase in end-plate thickness, from 16 mm to 32 mm, has a little effect on the connection capacity. For larger bolt diameters (M24 and M27), M_y and M_u increase by 900% and 225%, respectively, as end-plate thickness increases from 8 mm to 24 mm; then, the behavior turns to thick plate and the increase is negligible from 24 mm to 32 mm. This is because when the behavior changes to thick plate behavior, the bolts yielding and rupture controls the behavior of the connection, and the increase in end-plate thickness has no significant effect.

4.3. Bolt diameter (d_b)

Figs. 19–22 show yield and ultimate moments against bolt diameter for both four bolts and multiple row configurations, respectively. For thinner end plates (8 and 12 mm), the yield moment increases by only 10% despite of the increase in bolts diameter, from 12 mm to 27 mm, because the yielding is due to end-plate yielding only. The connection ultimate moment shows increase up to about 300%, which has not been shown for yield moment, when the bolt diameter is increased from 12 mm to 24 mm. This is due to the relatively large post-yielding capacity of the end plate which allows bolts to achieve more capacity. Further increase from 24 mm to 27 mm does not increase the ultimate moment as the end plate has reached its ultimate capacity.

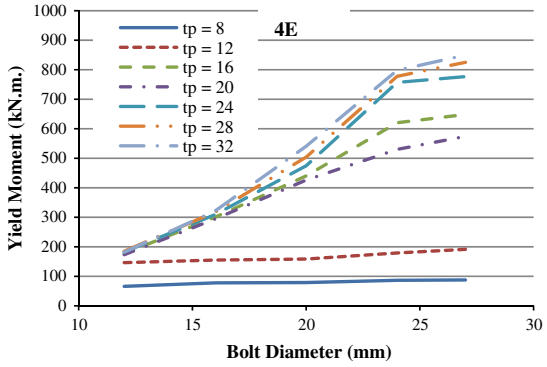

Figure 19 Four bolts configuration yield moment vs. bolt diameter.

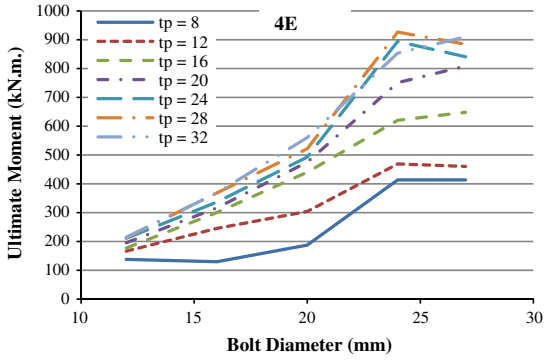

Figure 20 Four bolts configuration ultimate moment vs. bolt diameter.

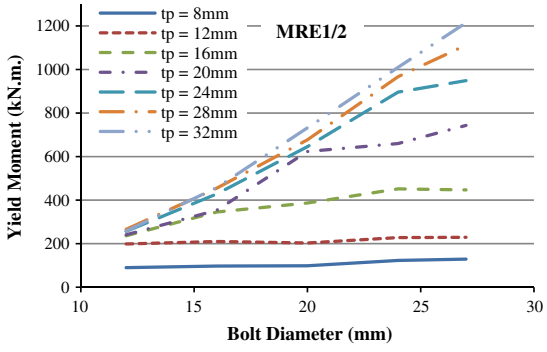

Figure 21 Multiple row configuration yield moment vs. bolt diameter.

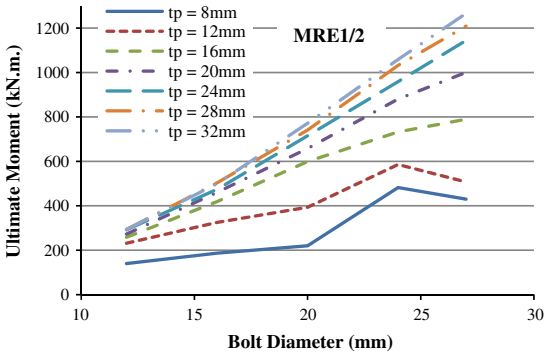

Figure 22 Multiple row configuration ultimate moment vs. bolt diameter.

For thicker end plates (24–32 mm), the yielding and ultimate moments increase by about 400–450% when bolt diameter changes from 12 mm to 24 mm. Increasing the bolt diameter from 24 mm to 27 mm has almost no effect on the yield moment. This is because for diameters smaller than M24, these thicknesses act as thick plate and the yielding is due to bolts only, while for diameters larger than M24, these thicknesses act as thin plate and the yielding is due to end-plate yielding.

4.4. Bolts gage (g)

Figs. 23 and 24 show yield and ultimate moments against bolts gage for both four bolts and multiple row configurations, respectively. The increase in bolts gage from 60 mm to 100 mm decreases the ultimate and yield moments by 20% for 4E configuration and 40% for MRE1/2 configuration. This is due to the decrease in end-plate stiffness which increases the prying forces in bolts decreasing their moment capacity. Further increase in bolts gage from 100 mm to 140 mm has much smaller effect on the connection capacity as effect of the gage on the end-plate capacity decreases.

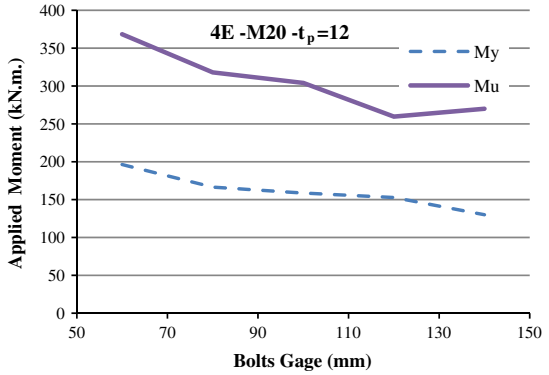

Figure 23 Four bolts configuration yield and ultimate moment vs. bolts gage.

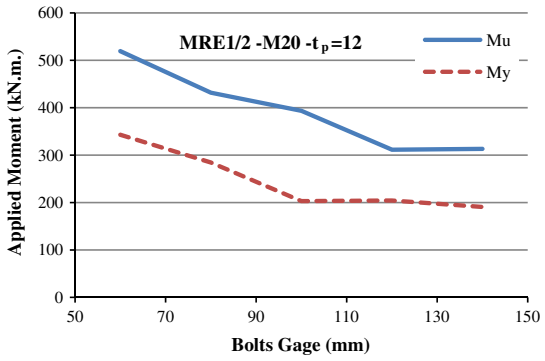

Figure 24 Multiple row configuration yield and ultimate moment vs. bolts gage.

4.5. Bolts inside and outside pitch (p_i, p_o) and inner bolts pitch (p)

Fig. 25 shows yield and ultimate moments against bolts inside and outside pitch, while Fig. 26 shows yield and ultimate moments against inner bolts pitch for both four bolts and multiple row configurations, respectively. By the increase in bolts pitch from 30 mm to 50 mm, both connection ultimate and yield moments decreased by 40–45% due to the decrease in end-plate bending capacity which leads to earlier formation of prying forces in the bolts decreasing their capacity. Further increase, from 50 mm to 70 mm, has a very little effect because

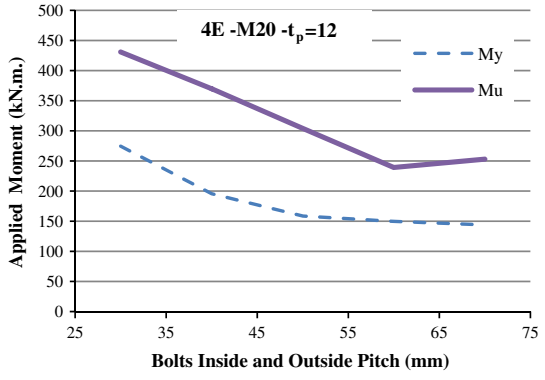

Figure 25 Four bolts configuration yield and ultimate moment vs. bolts inside and outside pitch.

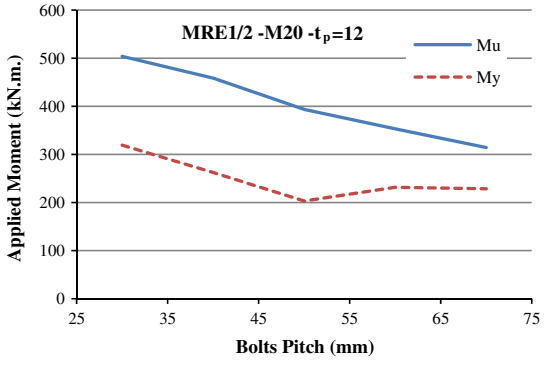

Figure 26 Multiple row configuration yield and ultimate moment vs. inner bolts pitch.

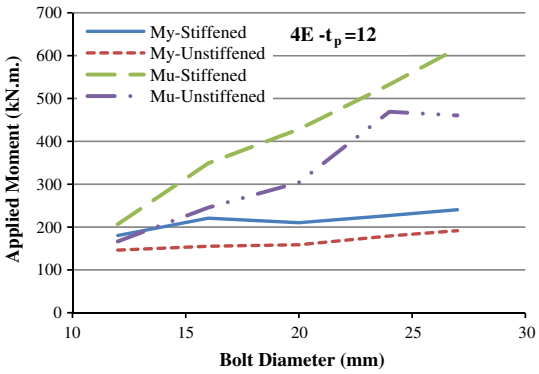

Figure 27 Four bolts configuration yield and ultimate moments vs. bolt diameter with and without end-plate stiffener.

the connection behavior has turned to thin plate behavior where it is controlled by the end-plate bending only.

4.6. End-plate stiffener

Fig. 27 shows yield and ultimate moments against bolts diameter for four bolts (both stiffened and unstiffened) and Fig. 28 shows yield and ultimate moments against end-plate thickness for multiple row configuration (both stiffened and unstiffened). It was noted that the stiffeners greatly increase the end-plate yielding capacity for both end-plate configurations, while it has a very little effect on the yielding and rupture of bolts. The end-plate stiffeners increase both the connection yielding and the ultimate moments with about 30% where connection acts as thin plate. The percentage of increase decreases as the connection's behavior tends to be thick plate. This increase in the yield moment may change the connection behavior from thin to thick behavior.

5. Simplified design procedures

The behavior of the end-plate connections is very complex, but in general, two limit states control the behavior of the end-plate connection which are the end-plate yielding and bolt rupture. In this study, the thick plate behavior will be adopted to develop simplified design procedures for the end-plate connection. Borgsmiller determined experimentally a threshold between thick and thin plate behavior to be at the point where ninety percent of the end-plate bending strength is achieved. So, the end plate will be designed to 111% of the design moment to assure thick plate behavior.

5.1. End-plate strength

The end-plate bending strength is determined using yield line analysis which estimates the yielding moment of the end plate. The application of yield line theory to determine the strength of an end plate requires three basic steps: detection of a yield line pattern, generation of equations for internal and external work, and solution of internal and external work equality.

The internal work stored within a yield line pattern is the sum of the internal work stored in each of the yield lines forming the mechanism. For simplicity, it is convenient to break the

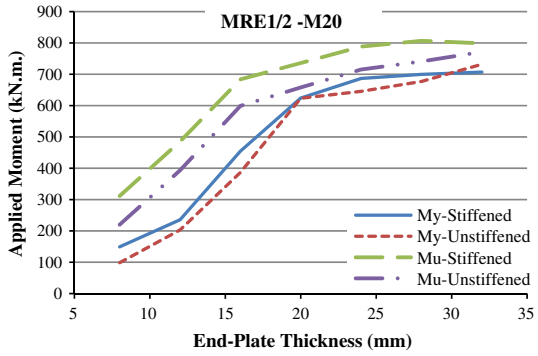

Figure 28 Multiple row configuration yield and ultimate moments vs. end-plate thickness with and without end-plate stiffener.

internal work components down into Cartesian x and y components. The general expression for internal work stored by the yield line pattern is as follows:

$$Wi = \sum_{n=1}^{N} (m_p \theta_{nx} l_{nx} + m_p \theta_{ny} l_{ny}) \tag{1}$$

where θ_{nx} and θ_{ny} are the x and y components of the relative rotation of the rigid plate segments along the yield line, l_{nx} and l_{ny} are the x and y components of the yield line length, and m_p is the plastic moment strength of the plate per unit length,

$$m_p = F_y \frac{t_p^2}{4} \tag{2}$$

The external work due to the unit virtual displacement is given by the applied tension flange force by the virtual displacement.

$$We = \frac{M_{pl}}{d} \delta \tag{3}$$

where M_{pl} is the end-plate yielding moment, δ is the applied virtual displacement, and d is the distance from the centerline of the compression flange to the tension side edge of the end plate for simplicity taken equal to beam depth.

The end-plate stresses are monitored during the finite element analysis as shown in Fig. 29, and the yield line patterns in Fig. 30 were observed for different end-plate configurations. These patterns were analyzed by the virtual work method and solved for the plate bending capacity.

For the four bolts extended unstiffened end-plate configuration, the internal work is calculated for the pattern to accommodate for the applied virtual displacement at the tension flange δ.

$$Wi = F_y \frac{t_p^2}{4} \delta \left[\frac{2b_p}{p_o - d_b/2} + \frac{2b_p}{p_i - d_b/2} + 2\frac{2(p_i + g/\sqrt{2})}{g/2 - d_b/2} \right] \tag{4}$$

By equating the external work (3) and internal work (4) and rearranging for M_{pl}, we can get:

$$M_{pl} = F_y \frac{t_p^2}{4} d \left[\frac{2b_p}{p_o - d_b/2} + \frac{2b_p}{p_i - d_b/2} + 2\frac{2(p_i + g/\sqrt{2})}{g/2 - d_b/2} \right] \tag{5}$$

Similarly, the internal and external work are calculated and equated for the four studied configurations then rearranged for M_{pl}, which results a general equation for the end-plate moment capacity as follows:

$$M_{pl} = F_y \frac{t_p^2}{4} d K_{pl} \tag{6}$$

where M_{pl} is the end-plate bending strength, F_y is the end-plate yield stress, t_p is the end-plate thickness, d is the beam depth, and K_{pl} is the plate constant and changes according to the end-plate configuration given in Table 4.

5.2. Bolt strength

As the end-plate design considered the plate to be always "thick," this will ensure that the end plate remains elastic and that the bolts are not subjected to any significant prying forces. The elastic assumption that plane sections remain plane indicates that the outermost bolts will reach their tensile strength first. The outermost bolts are assumed to reach their ultimate force, while forces in inner bolts can be calculated

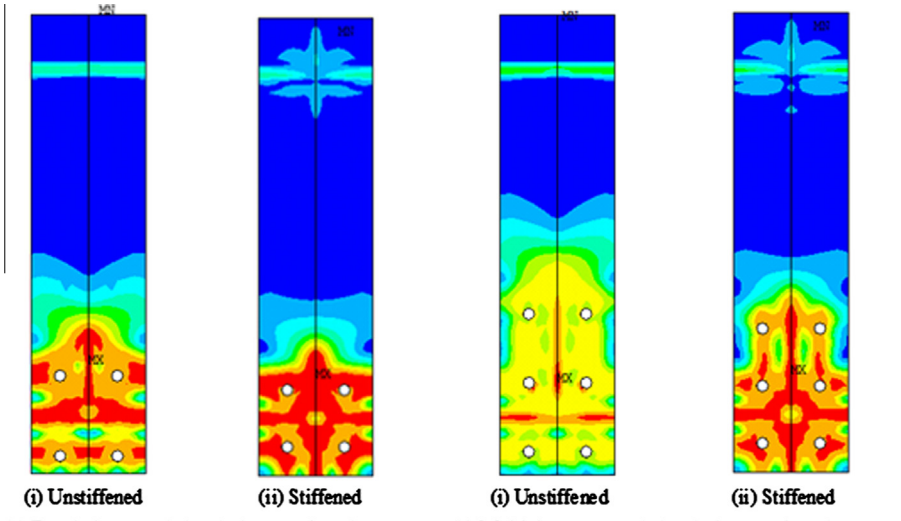

Figure 29 Monitored end-plate stresses at connection yield moment during finite element analysis for different configurations.

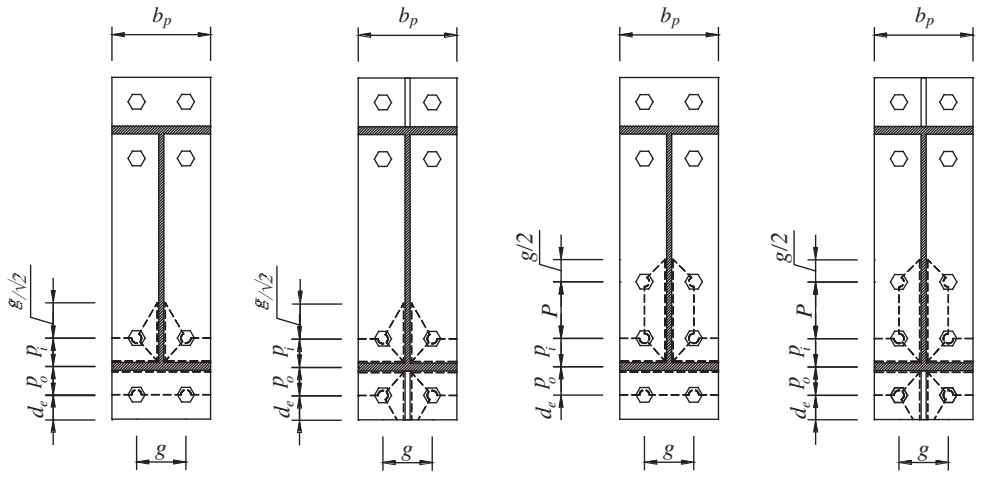

(a) Four bolts extended end plate yield line patterns (b) Multiple row extended end plate yield line patterns

Figure 30 Observed yield line patterns from finite element analysis.

Table 4 Plate constant K_{pl}.

Parameter		Plate constant K_{pl}
Four bolts extended end plate	Unstiffened	$K_{pl} = \frac{2b_p}{p_o - d_b/2} + \frac{2b_p}{p_i - d_b/2} + 2\frac{2(p_i + g/\sqrt{2})}{g/2 - d_b/2}$
	Stiffened	$d_e > g/\sqrt{2}$
		$K_{pl} = \frac{2b_p}{p_o - d_b/2} + \frac{2b_p}{p_i - d_b/2} + 2\frac{2(p_i + p_o + g\sqrt{2})}{g/2 - d_b/2}$
		$d_e < g/\sqrt{2}$
		$K_{pl} = \frac{2b_p}{p_o - d_b/2} + \frac{2b_p}{p_i - d_b/2} + 2\frac{2(p_i + p_o + d_e + g/\sqrt{2})}{g/2 - d_b/2}$
Multiple row extended end plate	Unstiffened	$K_{pl} = \frac{2b_p}{p_o - d_b/2} + \frac{2b_p}{p_i - d_b/2} + 2\frac{2\left(p_i + p + \frac{g}{2}\right)}{g/2 - d_b/2}$
	Stiffened	$d_e > g/\sqrt{2}$
		$K_{pl} = \frac{2b_p}{p_o - \frac{d_b}{2}} + \frac{2b_p}{p_i - \frac{d_b}{2}} + 2\frac{2\left(p_i + p_o + p + \frac{g}{2} + \frac{g}{\sqrt{2}}\right)}{g/2 - d_b/2}$
		$d_e < g/\sqrt{2}$
		$K_{pl} = \frac{2b_p}{p_o - \frac{d_b}{2}} + \frac{2b_p}{p_i - \frac{d_b}{2}} + 2\frac{2\left(p_i + p_o + p + d_e + \frac{g}{\sqrt{2}}\right)}{g/2 - d_b/2}$

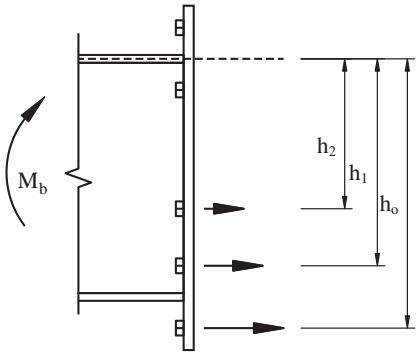

Figure 31 Bolts forces design model.

by linear distribution. Therefore, the connection strength, based upon bolt tension rupture (M_b), becomes the static moment of the relevant bolts strengths about the centerline of the compression flange (Fig. 31) and expressed by:

$$M_b = n(F_{ub}A_s)\sum_{i=0}^{N}\frac{h_i^2}{h_o} \tag{7}$$

where M_b is the bolt strength, n is the number of bolts in each row, ϕ_t is the is the tension resistance factor according to the (ECP-2008) = 0.70, F_{ub} is the bolts ultimate strength, A_s is the bolt stress area, N is the number of bolt rows, and h_i is the distance from the centerline of the compression flange to the centerline of the bolt row.

The connection nominal moment (M_n) is the minimum of both the plate strength (M_{pl}) and the bolts strength (M_b).

5.3. General formula for end-plate thickness (t_p)

In order to obtain a direct equation for the end-plate thickness, Eq. (6) was rearranged for end-plate thickness and substituting 111% of the factored design moment ($1.11\gamma iMi$) for plate yielding moment (M_{pl}).

$$t_p = \sqrt{\frac{4(1.11\gamma_i M_i)}{\phi_b F_y d K_{pl}}} \tag{8}$$

where $\gamma_i M_i$ is the connection factored design moment, ϕ_b is the is the flexural resistance factor according to the (ECP-2008) = 0.85.

6. Comparison with finite element analysis and current design procedures

To compare the proposed equations to the finite element results, it was necessary to determine the nominal (failure) moment from the finite element analysis. One of the two different reported moments for each sample, M_y or M_u, is considered the failure moment depending on its behavior. For thin plate connections, yield moment (M_y) is considered the failure moment because connections displaying this type of behavior would experience large deformations under working loads if the failure moment was assumed to be the ultimate moment (M_u). Thick plate connections would experience relatively acceptable deformations under working loads if the failure moment is assumed to be the ultimate moment (M_u). Therefore, it was necessary to set a numerical threshold to determine the failure moment. Borgsmiller set the following threshold to determine the nominal (failure) moment (M_n) of the connection.

$$M_n = M_y \quad if\ M_y < 0.75M_u$$

$$M_n = M_u \quad if\ M_y > 0.75M_u$$

The proposed design equations' predictions are compared to the finite element study results, the AISC equations in AISC-DG#16 [13], and to the ECP-2008. In the comparison of the AISC to the proposed equations, AISC-DG#16 and ECP-2008 are used without the resistance factors in order to be valid to compare to the finite element analysis results.

By comparing the yield line patterns observed from finite element analyses shown in Fig. 30 to those used in AISC_DG#16, two main differences were observed. The first difference is the horizontal yield lines in the AISC-DG#16 patterns which were not observed in the finite element analysis at the yielding point of the connection but appeared later at the connection ultimate moment. This is due to the fact that the AISC-DG#16 patterns were observed from experimental tests, which means it was not observed at the connection yield moment, but at the ultimate moment. The second difference is that the AISC-DG#16 patterns consider the bolts as infinite points, where the observed patterns show formation of circular yield lines around the bolt holes, and that the rotation of the rigid plates around the bolt occurs about these circular lines not around the center of the bolt. Therefore, the predicted connection capacity (for thin plate connections) by AISC is constant regardless of the bolt diameter, which is the same for ECP-2008. This was found to be conservative as by the increase in the bolt diameter, more fixation is provided to the end plate due to increased pretension force as well as reducing the rotation arm of the rigid panels rotating around the bolts, which increases the work done by these panels to rotate and accommodate for the applied virtual displacement. This leads

Table 5 Four bolts extended unstiffened comparisons.

Test Id 4E-d_b–t_p–d (Notes)	ECP-LRFD	AISC-DG16	Proposed EQ	Proposed F.E.A.	ECP-LRFD/ F.E.A.	AISC-DG16/ F.E.A.	Proposed EQ/ F.E.A.
	M_n (kN m)	M_n (kN m)	M_n (kN m)	M_n (kN m)			
4E-20-8-600	30	68	74	79	0.38	0.87	0.94
4E-20-16-600	126	274	296	319	0.40	0.86	0.93
4E-20-24-600	323	580	561	493	0.68	1.18	1.14
4E-20-32-600	420	580	561	560	0.78	1.03	1.00
4E-12-8-600	30	68	67	66	0.45	1.04	1.02
4E-12-16-600	126	209	202	177	0.79	1.18	1.14
4E-12-24-600	150	209	202	211	0.82	0.99	0.96
4E-12-32-600	172	209	202	215	0.94	0.97	0.94
4E-16-8-600	30	68	70	78	0.38	0.88	0.91
4E-16-16-600	126	274	281	300	0.46	0.91	0.94
4E-16-24-600	266	371	359	336	0.86	1.10	1.07
4E-16-32-600	305	371	359	368	0.95	1.01	0.97
4E-24-8-600	30	68	78	87	0.34	0.79	0.90
4E-24-16-600	126	274	311	316	0.40	0.87	0.99
4E-24-24-600	323	616	700	894	0.43	0.69	0.78
4E-24-32-600	420	835	807	853	0.53	0.98	0.95
4E-27-8-600	30	68	81	88	0.34	0.78	0.92
4E-27-16-600	126	274	324	319	0.40	0.86	1.02
4E-27-24-600	323	616	729	841	0.42	0.73	0.87
4E-27-32-600	420	1057	1022	910	0.49	1.16	1.12
4E-20-12-600 (g = 60)	68	182	200	196	0.35	0.93	1.02
4E-20-12-600 (g = 140)	68	140	155	130	0.52	1.08	1.19
4E-20-12-600 (p = 30)	N.A.	204	260	275	N.A.	0.74	0.95
4E-20-12-600 (p = 70)	N.A.	135	142	144	N.A.	0.94	0.99
4E-20-12-400	28	86	95	106	0.27	0.81	0.90
4E-20-12-700	50	159	166	198	0.25	0.81	0.84
4E-20-32-400	153	387	353	384	0.47	1.01	0.92
4E-20-32-700	269	677	646	650	0.43	1.04	0.99
				Mean	0.52	0.94	0.98
				Standard deviation	0.20	0.12	0.09

Table 6 Four bolts extended stiffened comparisons.

Test Id 4ES-d_b–t_p–d	ECP-LRFD	AISC-DG16	Proposed EQ	Proposed F.E.A.	ECP-LRFD/F.E.A.	AISC-DG16/F.E.A.	Proposed EQ/F.E.A.
	M_n (kN m)	M_n (kN m)	M_n (kN m)	M_n (kN m)			
4ES-12-12-600	N.A.	209	194	207	N.A.	1.01	0.94
4ES-16-12-600	N.A.	217	208	221	N.A.	0.98	0.94
4ES-20-8-600	N.A.	96	97	103	N.A.	0.93	0.94
4ES-20-12-600	N.A.	217	218	210	N.A.	1.03	1.04
4ES-20-16-600	N.A.	385	388	366	N.A.	1.05	1.06
4ES-20-20-600	N.A.	580	539	551	N.A.	1.05	0.98
4ES-20-24-600	N.A.	580	539	564	N.A.	1.03	0.96
4ES-20-28-600	N.A.	580	539	592	N.A.	0.98	0.91
4ES-20-32-600	N.A.	580	539	587	N.A.	0.99	0.92
4ES-24-12-600	N.A.	217	230	227	N.A.	0.95	1.01
4ES-27-12-600	N.A.	217	239	240	N.A.	0.90	0.99
				Mean	N.A.	0.99	0.97
				Standard deviation	N.A.	0.05	0.05

Table 7 Multiple row 1/2 extended unstiffened comparisons.

Test Id MRE-d_b–t_p–d (Notes)	ECP-LRFD	AISC-DG16	Proposed EQ	Proposed F.E.A.	ECP-LRFD/ F.E.A.	AISC-DG16/ F.E.A.	Proposed EQ/ F.E.A.
	M_n (kN m)	M_n (kN m)	M_n (kN m)	M_n (kN m)			
MRE 1/2-12-8-600	N.A.	81	84	90	N.A.	0.90	0.93
MRE 1/2-12-16-600	N.A.	287	258	258	N.A.	1.11	1.00
MRE 1/2-12-24-600	N.A.	287	258	292	N.A.	0.98	0.88
MRE 1/2-12-32-600	N.A.	287	258	293	N.A.	0.98	0.88
MRE 1/2-16-8-600	N.A.	81	96	97	N.A.	0.83	0.99
MRE 1/2-16-16-600	N.A.	324	383	419	N.A.	0.77	0.91
MRE 1/2-16-24-600	N.A.	510	459	474	N.A.	1.08	0.97
MRE 1/2-16-32-600	N.A.	510	459	499	N.A.	1.02	0.92
MRE 1/2-20-8-600	N.A.	81	101	98	N.A.	0.82	1.02
MRE 1/2-20-16-600	N.A.	324	402	387	N.A.	0.84	1.04
MRE 1/2-20-24-600	N.A.	729	717	715	N.A.	1.02	1.00
MRE 1/2-20-32-600	N.A.	797	717	771	N.A.	1.03	0.93
MRE 1/2-24-8-600	N.A.	81	106	123	N.A.	0.66	0.86
MRE 1/2-24-16-600	N.A.	324	424	452	N.A.	0.72	0.94
MRE 1/2-24-24-600	N.A.	729	953	959	N.A.	0.76	0.99
MRE 1/2-24-32-600	N.A.	1148	1033	1059	N.A.	1.08	0.98
MRE 1/2-27-8-600	N.A.	81	110	129	N.A.	0.63	0.85
MRE 1/2-27-16-600	N.A.	324	441	447	N.A.	0.72	0.99
MRE 1/2-27-24-600	N.A.	729	992	1144	N.A.	0.64	0.87
MRE 1/2-27-32-600	N.A.	1296	1307	1266	N.A.	1.02	1.03
MRE 1/2-20-12-600 (g = 60)	N.A.	231	313	343	N.A.	0.67	0.91
MRE 1/2-20-12-600 (g = 140)	N.A.	160	197	191	N.A.	0.84	1.03
MRE 1/2-20-12-600 (p = 70)	N.A.	223	299	319	N.A.	0.70	0.94
MRE 1/2-20-12-600 (p = 60)	N.A.	171	223	229	N.A.	0.75	0.98
MRE 1/2-20-12-400	N.A.	114	138	145	N.A.	0.79	0.95
MRE 1/2-20-12-700	N.A.	216	242	241	N.A.	0.90	1.01
MRE 1/2-20-32-400	N.A.	507	433	498	N.A.	1.02	0.87
MRE 1/2-20-32-700	N.A.	942	863	902	N.A.	1.05	0.96
				Mean	N.A.	0.87	0.96
				Standard deviation	N.A.	0.14	0.06

to larger end-plate capacity at the same plate thickness by increasing the used bolt diameter. The proposed equations consider this increase by incorporating the bolts diameter in the calculation of the end-plate capacity.

Tables 5–8 show a full comparison, for some of the study results, which includes the sample identification, the predicted nominal connection moment using ECP-LRFD, AISC Design Guide No. 16 (where applicable), and the proposed design equations as well as the proposed finite element nominal moment. Also, are shown the ECP-LRFD predictions to the finite element results ratio, the AISC-DG#16 predictions to finite element results ratio, and the proposed equations' predictions to finite element results ratio. The AISC-DG#16 predictions to finite element results ratio seem to have some discrepancies showing ratios ranging from 0.63 to 1.18, but it is noteworthy that 75% of them lie between 0.85 and 1.10. The ECP-LRFD

Table 8 Multiple row 1/2 extended stiffened comparisons.

Test Id MRES-d_b–t_p–d	ECP-LRFD M_n (kN m)	AISC-DG16 M_n (kN m)	Proposed EQ M_n (kN m)	Proposed F.E.A. M_n (kN m)	ECP-LRFD/ F.E.A.	AISC-DG16/ F.E.A.	Proposed EQ/F.E.A.
MRES-12-12-600	N.A.	N/A	245	211	N.A.	N/A	1.16
MRES-16-12-600	N.A.	N/A	257	277	N.A.	N/A	0.93
MRES-20-8-600	N.A.	N/A	120	149	N.A.	N/A	0.81
MRES-20-12-600	N.A.	N/A	270	236	N.A.	N/A	1.15
MRES-20-16-600	N.A.	N/A	480	455	N.A.	N/A	1.06
MRES-20-20-600	N.A.	N/A	717	736	N.A.	N/A	0.97
MRES-20-24-600	N.A.	N/A	717	788	N.A.	N/A	0.91
MRES-20-28-600	N.A.	N/A	717	807	N.A.	N/A	0.89
MRES-20-32-600	N.A.	N/A	717	799	N.A.	N/A	0.90
MRES-24-12-600	N.A.	N/A	284	287	N.A.	N/A	0.99
MRES-27-12-600	N.A.	N/A	296	334	N.A.	N/A	0.89
			Mean		N.A.	N/A	0.97
			Standard deviation		N.A.	N/A	0.11

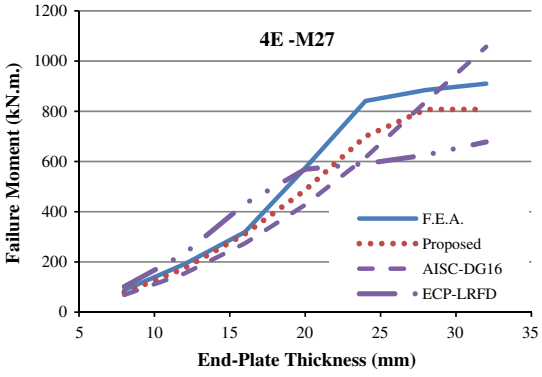

Figure 32 Connection nominal moment against end-plate thickness for the three procedures.

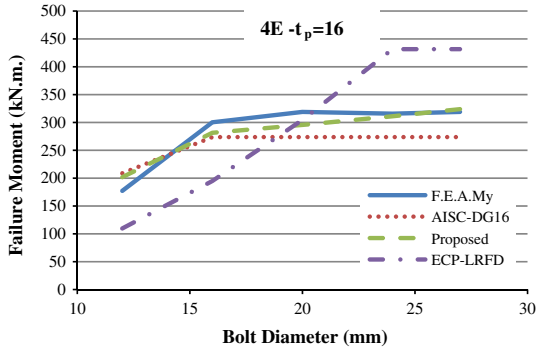

Figure 33 Connection nominal moment against bolt diameter for the three procedures.

predictions to finite element results ratio show that the ECP-LRFD predictions are very conservative, showing a mean ratio of 0.52.

Figs. 32–34 show the nominal moment obtained by the three procedures and observed from finite element analysis. Generally, the proposed equations show better correlation to the finite element results than the AISC-DG#16 and ECP-2008 equations.

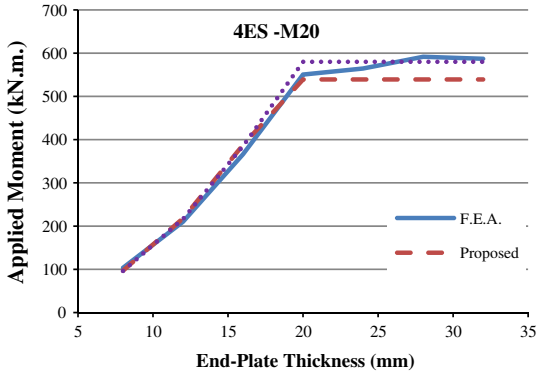

Figure 34 Connection nominal moment against end-plate thickness for the three procedures.

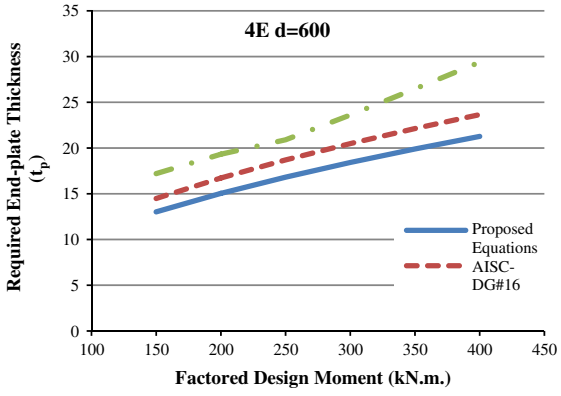

Figure 35 Required end-plate thickness by proposed equations, AISC-DG#16 and ECP-LRFD for different design moments.

Figs. 35 and 36 show the required end-plate thickness and bolts diameter, respectively, against the applied design factored moment using the proposed equations, AISC-DG#16 equations, and ECP-LRFD equations. The figures show that the proposed equations are more economic than the current codes design equations.

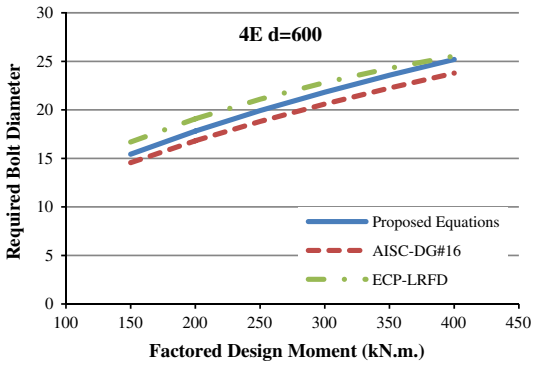

Figure 36 Required bolt diameter by proposed equations, AISC-DG#16 and ECP-LRFD for different design moments.

7. Conclusions

In this paper, a three-dimensional finite element model was presented to model the non-linear behavior of the extended end-plate moment connections. A parametric study was conducted on two end-plate configurations: four bolts and multiple row extended end plates. During the study, the distribution of stresses in the end plates was monitored, and yield line patterns were observed for each configuration. These yield line patterns were analyzed, and new design equations were proposed and compared to the finite element analysis results and to the current design codes equations. From the study, the following can be concluded:

- The multiple row extended end-plate configuration has shown 30–35% increase in both yield and ultimate moments than four bolts extended end-plate configuration even in thin plate configurations, where failure is governed by end-plate capacity; this increase is due to the increase in number of fixation points of the end plate which leads to the formation of more plastic hinges and larger yielding capacity of the end plate.
- The end-plate stiffeners increase the end-plate bending capacity up to 30% in the thin plate connections.
- New design equations are proposed using yield line patterns based on end-plate stress distribution at the connection yield moment monitored in the finite element analyses. On the contrary, the AISC Design Guide No. 16 patterns were based on experimental results; thus, the end-plate post-yielding effects are included.
- The proposed yield line patterns account for the size of the bolts where the AISC-DG#16 patterns do not. AISC patterns consider the bolts as infinite points and do not consider any effect for the bolt size on the end-plate capacity, which was found to be conservative. By the increase in the bolt diameter, more fixation is provided to the end plate due to increased pretension force as well as reducing the rotation arm of the rigid panels rotating around the bolts.
- The proposed equations have shown better correlation to the finite element analysis results than the current codes regarding the thin end plates. This is due to the enhanced yield line patterns used.

References

[1] Krishnamurthy N, Graddy DE. Correlation between 2- and 3-dimensional finite element analysis of steel bolted end-plate connections. Comput Struct 1976;6(4–5/6):381–9.
[2] Kennedy NA, Vinnakota S, Sherbourne AN. The split-tee analogy in bolted splices and beam-column connections. In: Proceedings of the international conference: joints in structural steelwork: the design and performance of semi-rigid and rigid joints in steel and composite structures and their influence on structural behaviour, April 6–9, Teesside Polytechnic, Middlesbrough, Cleveland, England; 1981. p. 2.138–57.
[3] Borgsmiller JT. Simplified method for design of moment end-plate connections. M.Sc. thesis. Virginia Polytechnic Institute and State University, USA; 1995.
[4] Bahaari MR, Sherbourne AN. 3D simulation of bolted connections to unstiffened columns-I.T-stub connection. J Construct Steel Res 1996;40(2):169–87.
[5] Bahaari MR, Sherbourne AN. 3D simulation of bolted connections to unstiffened columns – II. Extended end-plate connections. J Construct Steel Res 1996;40(3):189–223.
[6] Mays TW. Application of the finite element method to the seismic design and analysis of large moment end-plate connections. PhD thesis. Virginia Polytechnic Institute and State University, USA; 2000.
[7] Sumner EA. Unified design of extended end-plate moment connections subject to cyclic loading. PhD thesis. Virginia Polytechnic Institute and State University, USA; 2003.
[8] Hassan NK. Proposed basis for end-plate design in moment connections. Sci Bull 2004;39(2):177–96 [Ain Shams University].
[9] Egyptian code of practice for steel construction (allowable stress design), 3rd ed.; 2001.
[10] Samaan RA. Behavior and design of steel I-beam-to-column rigid bolted connections. PhD thesis. Ain Shams University, Cairo, Egypt; 2010.
[11] ANSYS. Swanson analysis systems online manual, version 11.0, and theory reference.
[12] Egyptian code of practice for steel construction (load and resistance factor design), 1st ed.; 2008.
[13] AISC. Design Guide Series 16, flush and extended multiple-row moment end-plate connections, American Institute of Steel Construction, Chicago, IL; 2002.

Abdelrahim Khalil Dessouki Professor of Structural Engineering, Department of Civil Engineering, Faculty of Engineering, Ain Shams University. **Research interest:** Design and behavior of steel structures, Cold-formed steel design and behavior, Fatigue performance of metals. **Education:** Ph.D. Civil Engineering Department, University of Windsor, Canada, Jan. 1985.

Ahmed Hassan yousef Aly Associate Professor of Structural Engineering, Department of Civil Engineering, Faculty of Engineering, Ain Shams University. **Research interest:** Design and behavior of steel structures, Bolted connections, Hollow sections connections, Concrete-filled steel tube columns, Tubular structures. **Education:** Ph.D., Civil Engineering Department, Polytechnic University of Valencia, Spain, September 2002.

Mohamed Mostafa Mohamed Ibrahim Structural Engineer at Modern Engineering, Group Consultation Office. **Education:** MSc, Structural Engineering Department, Faculty of Engineering, Ain Shams University, Cairo, Egypt, March 2012.